Frequency-specific SSFP imaging of hyperpolarized ^{13}C compounds at 14.1T

Cornelius von Morze[1], Subramaniam Sukumar[1], Galen Reed[1], Peder E Larson[1], John Kurhanewicz[1], and Daniel B Vigneron[1]
[1]*Department of Radiology and Biomedical Imaging, UCSF, San Francisco, California, United States*

Introduction- A periodic train of RF pulses has a frequency response that is periodic with 1 / TR, resulting in signal modulation if TR ≤ T_2[1]. Most prior applications of SSFP to hyperpolarized imaging have not utilized its spectral selectivity. Either only a single metabolically inactive agent was imaged[2-4], or a uniform profile was assumed for multiple resonances[5]. In the limit of low flip angle, the off-resonant frequency response approximates a signal null. In this regime, frequency-specific images may be obtained with one acquisition per frequency. Metabolic imaging of [1-^{13}C]pyruvate co-polarized with [^{13}C]urea is a promising new method for characterization of tumor metabolism and perfusion simultaneously *in vivo*. The goal of this study was to demonstrate the feasibility of using SSFP at 14.1T for dynamic imaging of co-polarized pyruvate and urea at high spatiotemporal resolution.

Methods- *Simulations*- The transient frequency response of hyperpolarized magnetization to a series of RF pulses was computed. The Bloch equations were adapted to eliminate relaxation effects (no T_1 recovery, and no T_1 or T_2 decay for a short train). The magnetization was evolved over a series of 36 pulses by successive matrix multiplications[6], with TR = 1.44 ms and flip angle α= 0.4° – 0.8°, over a frequency range of ±0.5ppm. This TR was the shortest value above the minimum for 2.5mm resolution that maximized avoidance of integer multiples of 1 / TR (4.6ppm) among any peaks. Blurring effects were estimated by computing the point spread function (PSF) due to signal variation over the imaging pulses. For the dynamic scenario, relaxation processes were considered. *Hyperpolarization*- 30 mg 99% [1-^{13}C]pyruvic acid (neat) and 55 mg 99% [^{13}C]urea (6.4M in glycerol), both mixed with trityl radical and 1.0-1.5 mM Dotarem, were loaded into the Hypersense DNP polarizer. The mouse was injected with 350 µL 80 mM solution (approx. equimolar for pyruvate and urea) over 12 sec. Imaging started 18 sec after injection. *Scans*- The sequence was implemented on a 14.1T Varian 600WB micro-imaging system, equipped with 55mm 100G/cm gradients. A product 2D balanced SSFP ('trueSSFP') pulse sequence was modified to run dynamically, and to cycle between three center frequencies (pyruvate, lactate, urea) at each timepoint. Two phantom experiments were conducted. First, two syringe phantoms (i.d.= 3 mm) containing enriched [^{13}C]urea (8M) and [1-^{13}C]lactate (5.5M), respectively, were scanned. Second, a co-polarized solution of pyruvate and urea (40 mM) was transferred to a NMR tube (i.d.= 9 mm) and scanned dynamically every 3 seconds over 87 seconds. Parameters: TE / TR = 0.72 ms / 1.44 ms, flip angle= 0.6°, matrix= 24 x 24, FOV= 6 cm, resolution= 2.5 mm x 2.5 mm, slice= 10 mm, dummy cycles= 12, RF pulse= 100 µs Gaussian, scan duration= 52 ms per frequency. A spoiling delay of 200 ms was programmed between frequencies. A normal mouse kidney was also imaged dynamically. The pyruvate center frequency was determined and set automatically by homebuilt scanner software, using a 1° spectrum from the imaged slice, acquired just prior to imaging. Urea and lactate were set with fixed offsets.

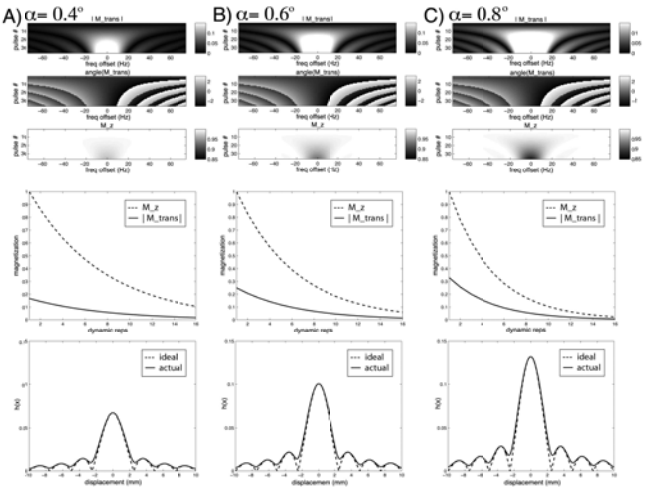

Fig. 1- Response of hyperpolarized magnetization to a series of RF pulses with varying small flip angles (col. A-C), TR= 1.44ms. Top row: Transverse magnitude/phase and Mz, as function of frequency offset. Middle row: Dynamic hyperpolarized signal, Δt=3 sec and T_1= 20 sec. Bottom row: Point spread function h(x) due to signal variation during train.

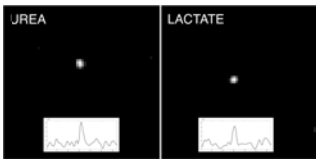

Fig. 2- SSFP images of thermal urea (left) and lactate (right) syringes, created by moving the RF center frequency.

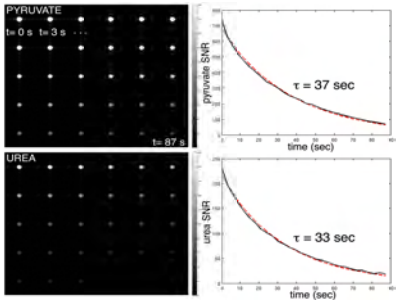

Fig. 3- Dynamic SSFP images of 40mM solution of co-polarized pyruvate (top) and urea (bottom). Plots show image SNR and exponential fits to the data.

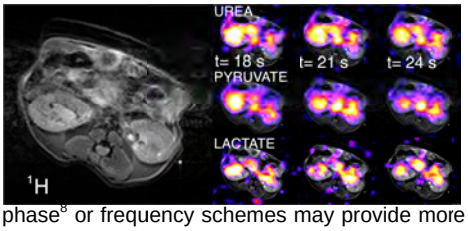

Fig. 4- Dynamic SSFP imaging of hyperpolarized ^{13}C compounds in mouse kidney.

Results- *Simulations*- The frequency response has narrow bands of increasing signal spaced by 1 / TR. Outside these bands, the pulses have little effect on the magnetization. In-band stability is improved by using a greater number of dummy cycles, but is traded against narrowing bandwidth. 12 dummy cycles and 24 phase steps produced reasonable results. The passband width of the frequency response is approximately 0.2 ppm (FWHM), which is tolerable given automatic setting of the center frequency, accounting for global B_0 shifts. For this train length, α=0.6° is roughly optimal for signal over 15-45 sec, assuming T_1= 20 sec. *Scans*- Results of the phantom imaging experiments are shown in Figures 2 & 3. Separate images of each thermal syringe were produced (SNR ~5:1), by changing the center frequency, with no detectable component at the position of the other syringe. For the hyperpolarized scan, high SNR dynamic images of the co-polarized pyruvate and urea were produced over 87 sec. The data fit well to decaying exponentials with time constants of 37 sec (pyruvate) and 33 sec (urea).

Discussion- We have demonstrated a new method utilizing the spectral selectivity of the SSFP response in the low flip angle regime for obtaining dynamic frequency-specific images of multiple hyperpolarized compounds at high spatiotemporal resolution. This approach avoids large tip refocusing pulses that may cause excessive losses of hyperpolarized magnetization due to miscalibration of transmit gain or spatial B_1 variation. Due to the narrow bandwidth of the response, automatic determination and setting of a reference center frequency is critical. Custom optimized SSFP acquisitions incorporating alternating TR[7] or variable RF phase[8] or frequency schemes may provide more bandwidth.

Acknowledgements- We acknowledge grant support from NIH P41EB013598-01.

References- 1. Freeman et al. *JMR*. 1971. 2. Golman et al. *PNAS*. 2003. 3. Svensson et al. *MRM*. 2003. 4. Johansson et al. *MRM*. 2004. 5. Leupold et al. *MAGMA*. 2009. 6. Pauly et al. *IEEE TMI*. 1991. 7. Leupold et al. *MRM*. 2006. 8. Grant et al. *Proc 19th ISMRM*. 2011.